

Study of excited states in ^{208}Pb by particle- γ coincidences with the $^{207}\text{Pb}(d,p)^{208}\text{Pb}$ and $^{209}\text{Bi}(t,\alpha)^{208}\text{Pb}$ reactions

M. Schramm, K. H. Maier, M. Rejmund, and L. D. Wood
Hahn-Meitner-Institut Berlin, Glienicker Str. 100, D-14109 Berlin, Germany

N. Roy, A. Kuhnert, A. Aprahamian, J. Becker, M. Brinkman, D. J. Decman, E. A. Henry, R. Hoff, D. Manatt,
 L. G. Mann, R. A. Meyer, W. Stoeffl, G. L. Struble, and T.-F. Wang
Lawrence Livermore National Laboratory, Livermore, California 94550

(Received 18 February 1997)

Excited states in ^{208}Pb have been studied by measuring γ rays in time coincidence with reaction charged particles. ^{208}Pb states were produced with both the $^{207}\text{Pb}(d,p)^{208}\text{Pb}$ and $^{209}\text{Bi}(t,\alpha)^{208}\text{Pb}$ reactions. The energy resolution of the particle spectra of 100 keV allowed a rough determination of level excitation, which then was determined with high resolution from the coincident γ decay measured in Ge detectors. Many new γ transitions have been found and previously unresolved multiplets of states resolved. The data give spectroscopic factors for neutron transfer and proton pickup. Spins and parities of levels could be deduced from their γ decays. A least squares fit of all γ energies gave very precise (0.1 keV) level energies. All states predicted by the shell model below 4.6 MeV are now found and their spins determined unambiguously. [S0556-2813(97)03009-4]

PACS number(s): 21.60.Cs, 23.20.Lv, 25.45.Hi, 27.80.+w

I. INTRODUCTION

The experimental information on the properties of the excited states of ^{208}Pb is still scant, although it has been studied by a variety of reactions and techniques. The compilation of Martin [1] includes a very detailed study of the (p,p') reaction [2] and the relevant data from $^{207}\text{Pb}(d,p)^{208}\text{Pb}$ [3,4]. More recent work resulting with new information is the (e,e') study by Connelly *et al.* [5], a measurement of the $^{209}\text{Bi}(d,^3\text{He})^{208}\text{Pb}$ reaction by Grabmayr *et al.* [6], the measurement of γ rays from inelastic scattering of fast reactor neutrons by Govor *et al.* [7], and the study of γ transitions between high spin states by inelastic heavy ion scattering by Schramm *et al.* [8]. Around 5 MeV excitation energy in ^{208}Pb , the level density becomes so high that spectroscopy of charged particles often cannot resolve multiplets. Therefore it is difficult to relate states that are seen in different reactions, because (1) their energy is not determined precisely enough, and (2) often no other criterion like the spin of the states is available. High resolution, precision γ -spectroscopy can overcome part of these resolution problems. However little work of this kind has been done, except for the mentioned neutron and heavy ion scattering. A study of the β decay of ^{208}Tl provided decay information [9] on the low lying states with $I \leq 6$. In-beam work has been restricted to selected levels, because ^{208}Pb is too neutron rich to be reached by standard compound-nucleus reactions with light or heavy ions. Very recently γ transitions in ^{208}Pb have been measured using both the $^{207}\text{Pb}(d,p)^{208}\text{Pb}$ reaction and inelastic proton scattering through analog resonances to excite levels in ^{208}Pb . These measurements [10] also included γ - γ coincidences, but did not include particle spectra to identify the populated level, and concentrated on high energy γ transitions to the ground state.

Some of earlier limitations have been overcome in the present experiments by measuring particle- γ coincidences.

The particle energy is measured with moderate resolution (100 keV), sufficient to select the energy of the level that is populated. As a practical matter, levels degenerate in energy usually have different γ -decay patterns and can therefore be distinguished. Also, Ge detectors have been used to measure the γ rays with an energy resolution between 1 keV at 100 keV energy and 6 keV at 6 MeV. Two reactions were used, populating different states in ^{208}Pb : The $^{209}\text{Bi}(t,\alpha)$ reaction populates proton-proton hole states, with the particle in the $h_{9/2}$ orbital as in the ground state of ^{209}Bi . The results of this measurement are therefore spectroscopic factors for the proton pick up and the γ decay of these states. Similarly the reaction $^{207}\text{Pb}(d,p)$ excites exclusively neutron-neutron hole states with the hole in the $p_{1/2}$ orbital; again the spectroscopic factors and the γ decay are measured. Historically, proton- γ coincidences with the (d,p) reaction were already measured by Earle *et al.* [11] in 1970, but significantly improved results can be obtained with present detector technology.

In this work our experimental data are presented and the level scheme of ^{208}Pb is critically reviewed, where new data have become available. A part of the data have already been published [12], and the results of the $^{207}\text{Pb}(d,p\gamma)$ study are presented in detail in [13]. The completeness of these data allows to deduce strictly empirical wave functions for many states of ^{208}Pb [13], if the wave functions are restricted to one-particle-one-hole configurations. The matrix elements of the shell model Hamiltonian, the residual interaction, can then be calculated from the wave functions [14,15]. These conclusions are not part of the present work, but will be presented in a forthcoming publication [16].

II. THE $^{209}\text{Bi}(t,\alpha\gamma)^{208}\text{Pb}$ EXPERIMENT

A. Design of the experiment and procedures

The $^{209}\text{Bi}(t,\alpha\gamma)^{208}\text{Pb}$ reaction was used to excite levels in ^{208}Pb . Due to the huge positive energy balance of this

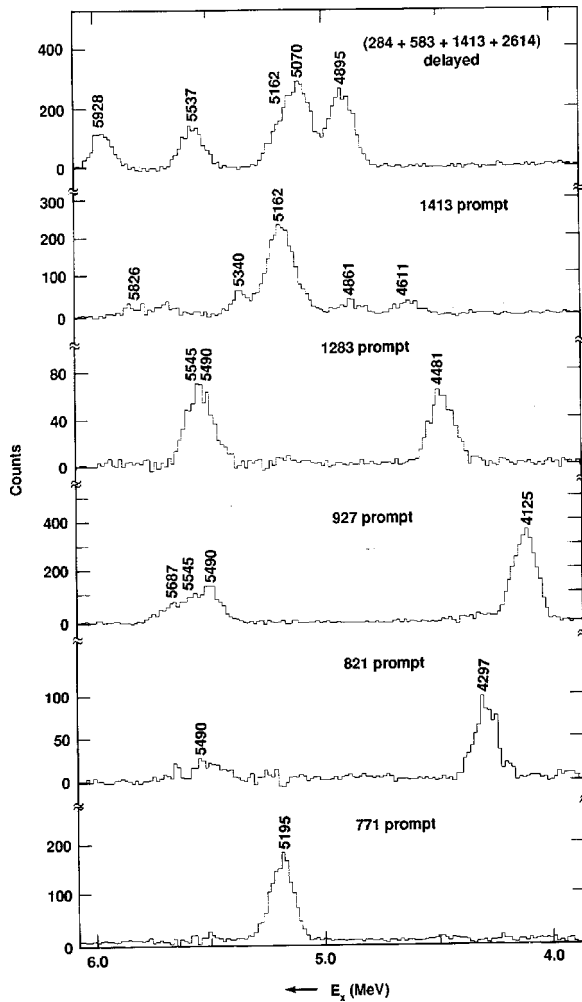


FIG. 1. α -particle spectra in coincidence with selected γ transitions. The abscissa gives the excitation energy in ^{208}Pb corresponding to the α energy.

reaction with $Q = +16$ MeV, the α particles are well separated in energy from any other charged particles. A distorted-wave Born approximation (DWBA) calculation of the α -particle angular distribution with the code DWUCK predicts that the α particles are emitted at backward angles at the chosen triton energy of 11.5 MeV. A measured angular distribution at $E_t = 12$ MeV [17] for $^{208}\text{Pb}(t, \alpha)$ agrees with this. Therefore α particles were detected with four trapezoidal Si detectors of 400 μm thickness, arranged symmetrically around the beam axis and perpendicular to it 3 cm from the target. The detectors covered the angular range from about 147° to 168° . The detection efficiency, taking into account the angular distribution of the α particles, was 15%. The halfwidth (FWHM) of the α lines in the interesting energy region (20–25 MeV) was better than 120 keV; kinematic broadening contributes about 80 keV, and the thickness of the 0.5 mg/cm^2 metallic Bi target around 50 keV to the energy resolution. The experiment was performed at the tandem accelerator of the Los Alamos National Laboratory. Three coaxial Ge(HP) detectors of 21% efficiency (relative to a $3'' \times 3''$ NaI crystal) each were placed at 90° and -70° in the horizontal plane facing the target and one at 90° above the target; the γ rays from the target had to enter the latter

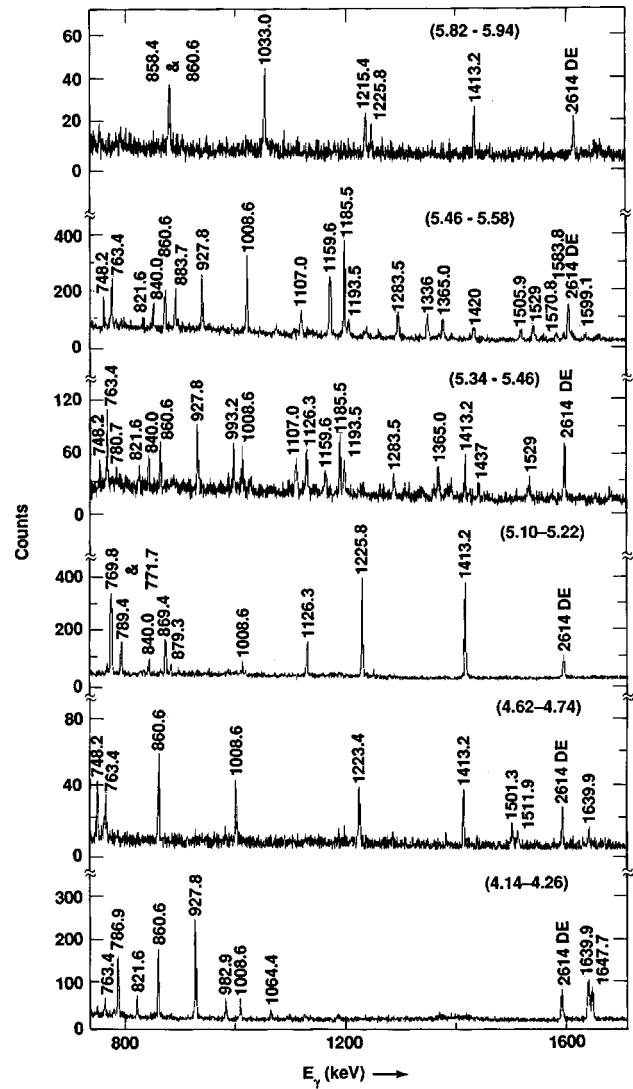


FIG. 2. Partial γ spectra in coincidence with α particles in selected energy windows. The range of excitation energy, corresponding to the α -energy window is indicated.

detector from the side. The target-detector distance was about 5 cm. The beam dump was a well-shielded Faraday cup about 1 m downstream from the target. All events in which one of the four α detectors was in coincidence with at least one γ detector were accepted. The coincidence time window amounted to $-100 \text{ ns} \leq t_\gamma - t_\alpha \leq 700 \text{ ns}$. Events written on tape consisted of α and γ energy and the time between α and γ signals. The energy range of the Ge detectors was limited to 4 MeV. Consequently γ transitions of higher energy and in particular from low spin states at higher energies that decay directly to the ground state are not included. The time resolution for all detector combinations was 5 ns at $E_\gamma = 1$ MeV. The contributions from all α and γ detectors have been added in the off line analysis; no significant α - γ angular correlation effects could be found by evaluating coincidences between α detectors in the same plane as the γ detector or perpendicular to it. Intensity relations were determined from the summed spectra.

With a typical beam current of 10 nA, the count rate for reaction α particles in each detector was about 40/s, the

γ -count rate 10 kHz, and the total α - γ coincidence rate 20/s. Approximately 3 million α - γ coincidences were recorded. The true-to-random ratio in the total coincident γ spectra was about 200, as deduced from the intensity ratio (1:10) of the 1181.4 keV line in ^{210}Po and the 583.2 keV line in ^{208}Pb as compared with their real ratio [18] of 20:1. The suppression of random events was at least one order of magnitude better for the smaller prompt time window as used in the off line evaluation. The efficiency of the Ge detectors was calibrated with sources of ^{133}Ba , ^{152}Eu , and ^{56}Co placed at the target position. Energy calibration of the γ spectra relied on the internal calibration, using the well-known contaminant lines from ^{210}Po and the 583.2 keV and 2614.5 keV transitions in ^{208}Pb . Small corrections for nonlinearities were taken from the source spectra.

The gain stability of the α detectors was checked during the measurements by the lines due to elastically scattered tritons and the α particles to the ground state of ^{208}Pb . Off line, a much better energy calibration was established from α spectra in coincidence with selected γ rays. Energies of the levels were determined to ≤ 5 keV from the centroids of the stronger α lines. The placement of γ transitions in the level scheme was restricted accordingly.

The requirement of an α - γ coincidence reduces the count rate of the wanted γ transitions only by a factor 6. The detection efficiency is therefore essentially that of a γ singles measurement. The background is very small, and therefore the γ decay of levels populated with ≤ 10 μb cross section was detected in favorable cases. We estimate that all γ transitions, produced with a cross section ≥ 20 μb , have been placed.

B. Data evaluation and construction of the level scheme

Strong γ rays were placed in the level scheme according to the following procedure: (i) The excitation energy of the directly populated states was determined from the α spectra in coincidence with these γ lines. (ii) γ spectra were sorted for narrow gates on the previously selected α transitions. (iii) The intensity balance in these spectra was used. The analysis proceeded from lower to higher excitation energies making use of the established decay patterns for the lower levels from either this analysis or previous work. Problems arose only when the data indicated that closely spaced levels (≤ 30 keV) decay to another set of levels with narrow spacing. For some states, Doppler broadening made the evaluation a little more difficult. Because γ rays were only recorded up to 4 MeV the decay of the low spin states above 4 MeV to the ground state could not be observed and γ transitions populating these levels not placed.

Figures 1 and 2 show examples of α spectra coincident with individual γ lines and γ spectra in coincidence with α particles in selected energy windows of 120 keV width. For instance, Figs. 1(c) and 1(d) show that a 1283 keV γ line occurs in the decay of a level at about 4481 keV and a 927 keV γ transition originates from a state at 4125 keV. It is clear that both these transitions populate the 5^- state at 3198 keV; the energies of its neighboring states at 2615 keV and 3475 keV are clearly incompatible with the measured α and γ energies. Therefore levels with precise energies of 4125.4

keV and 4480.8 keV are now established. Figures 1(c) and 1(d) show furthermore that these two γ rays are also coincident with α particles, populating states close to 5.5 MeV. Levels at 5490.3, 5542.0, and 5545.5 keV are strongly populated; the γ spectrum in coincidence with α particles of the appropriate energy [Fig. 2(b)] reveals then, for instance, a 1365 keV transition with the proper intensity to be assigned as connecting the 5490 keV and 4125 keV levels. Seven other decays can be assigned to this level, of which the 1107, 1193, 1283, 1529, and 1571 keV lines are in the presented part of the spectrum. The 1420 keV transition also populates the 4125 keV state; it originates from the 5545 keV level. The 1159.6 keV transition connects the 5542 and 4383 keV levels, and the following decay of this level shows up in the 1185 keV line. A difficult problem in this case is presented by the 1283 keV multiplet. A 1283.0 keV transition decays from the 4481 keV level, but two more lines at 1283.5 keV are assigned to decays from the 5490 and 5545 keV states. This leads to some uncertainty in the distribution of the observed total strength. All results on γ decays are summarized in Table V, a conventional drawing of a decay scheme would be too complicated. The evaluation of the lifetimes of the lowest 10^+ and 8^+ states and the γ transitions above the 10^+ isomer have already been presented in [12].

C. Results on reaction mechanism, cross sections, and spectroscopic factors

The (t, α) reaction at 11.5 MeV is a clean direct reaction and spectroscopic factors can be extracted. The proton-hole states in the ^{208}Pb core are $s_{1/2}$, $d_{3/2}$, $h_{11/2}$, and $d_{5/2}$. They combine with the $h_{9/2}$ proton of the ^{209}Bi ground state to give the levels that are expected to be populated in ^{208}Pb . Configuration mixing spreads the strength out over many more levels and the spectroscopic factors indicate the probability of the proton-proton-hole component.

Absolute cross sections for the strongest γ transitions in ^{208}Pb from the reactions of tritons with ^{209}Bi have been measured in a previous study [18]. Normalizing to these lines, the intensities of the measured α - γ coincidences in this experiment can be approximately converted into absolute cross sections, because the α - γ coincidence efficiency is roughly identical for all levels (see below); the cross section for the population of a level in μb is equal to the strength S_{expt} in Table V multiplied by 40 within about 50%. The (t, α) reaction at 11.5 MeV is a direct proton pickup reaction. Clear evidence for this is that some levels are not noticeably populated, as the 3920 keV 6^- state and the 4038 keV 7^- state. The observation limit for these levels is of the order of 1% of the strongest levels with the same spin. Alpha evaporation from the compound nucleus is therefore also limited to this fraction of the cross section. Further evidence for the direct nature of the (t, α) reaction is the good agreement of the spectroscopic factors with those from $(d, ^3\text{He})$ at 45 MeV [6]. A simple classical picture explains the effectiveness of this reaction. The incoming triton is slowed down by the Coulomb field, and it comes to rest at the nuclear surface. There it is transformed into an α particle, that gains twice the triton energy from acceleration by the Coulomb field. The

TABLE I. Spectroscopic factors from $^{209}\text{Bi}(t, \alpha \gamma)$ in comparison with the ($d, ^3\text{He}$) results of [6]. Spectroscopic factors from the present experiment (S) are compared with those from [6] (S_G). Our data are normalized for the various transferred j to those of [6] as indicated. The presented numbers are $(2I+1)S/(2I_{\text{target}}+1) = (2I+1)S/10$.

E^*	Spin	l	S	S_G	Comment	E^*	Spin	l	S	S_G	Comment
2615	3^-	2	0.096	0.12		5213	6^+	5	0.811	1.17	G :
3198	5^-	0	0.070	0.070	Normalized	5217	4^+	5	0.231		Doublet
3475	4^-	0	0.004	0.01		5234		5		0.26	Ident. 5239?
3708	5^-	0	0.359	0.36		5239			0.194		If $l=5$
		2	0.110	0.11		5274	3^-	2		0.02	
3947	4^-	0	0.726	0.71		5317	3^+	5	0.515	0.42	
		2	0.174	0.17		5339	8^+	5	0.445	0.52	
3961	5^-	0	0.475	0.46		5352		5		0.06	
		2	0.124	0.12		5381		5	0.039	0.20	or $l=2$?
3996	4^-	0	0.042	0.04		5384		2	0.240	0.10	or $l=5$?
4051	3^-	0		0.01		5473		5		0.47	
		2	0.021		$l=2$ because 3^-	5482	5^-	2	0.054		Sum
4125	5^-	0	0.039	0.03		5490	6^-	2	1.276	1.33	Normalized
		2	0.706	0.55		5537	10^+	5	0.289	0.54	G :
4180	5^-	0	0.015	0.01		5542	7^-	2	1.214	1.76	
		2	0.045	0.03		5545	5^-	2	0.948		Triplet
4206	6^-	2	0.068	0.05		5581		2		0.04	
4255	3^-	0		0.06	Incompatible spin	5627		5		0.11	
		2	0.37			5643		2		0.50	Corresp.
4262	4^-	0	0.06	0.0	G : doublet	5649	5^-	2	0.387		
		2	0.68	1.05	with 4255	5665	5^-	2		0.53	of levels
4297	5^-	0	0.089	0.07		5675	4^-	2	0.686		
		2	0.331	0.26		5680		2		0.54	unclear
4324	4^+	5	0.138	0.17		5687	6^-	2	0.209		
4359	4^-	0	0.022	0.02		5690	4^+	5	0.145	0.51	
		2	0.303	0.28		5695	7^-	2	0.149	0.06	
4383	6^-	2	1.24	1.24	Normalized	5710		5		0.40	
4424	6^+	5	0.247	0.27		5727		5		0.10	
4481	6^-	2	0.193	0.14		5753		5		0.08	
4611	8^+	5	0.229	0.19		5778	3^-	2	0.200	0.20	
4698	3^-	2	0.150	0.05	G :	5790		5		0.06	
4709	5^-	2	0.119	0.22	Unresolved	5826	8^+	5	0.095	0.19	
4711	4^-	2	0.024		triplet	5846	1^+	5		0.17	
4861	8^+	5	0.284	0.25		5873		5		0.06	
4895	10^+	5	0.564	0.61		5887		2	0.081	0.13	
4938	3^-	2	0.101	0.08	Add. line	5902		5		0.05	
5011	9^+	5	0.053			5928	10^+	5	0.278	0.29	
5069	10^+	5	0.564	0.74		5932	2^+	5		0.13	
5076			0.012		if $l=2$	6000		2		0.05	
5086	7^-	2	0.106	0.18		6082		2		0.01	
5093	8^+	5	0.349	0.21		6183		5		0.01	
5127	2^-	2		0.03		6250		2	0.038	0.07	
5162	9^+	5	1.710	1.71	Normalized	6340	3^-	2	0.018	0.	
5193	5^+	5	0.846	1.86	G :	6458		2		0.02	
5195	7^+	5	1.133		Doublet	6535		2	0.023	0.07	
						6615		2		0.03	
						7216		2?	0.011		If $l=2$

TABLE II. Spectroscopic factors from $^{209}\text{Bi}(t, \alpha\gamma)^{208}\text{Pb}$. The results are arranged for the j of the picked up proton and the spins I of the populated states. The energies E of the states, their deviation from the centroid ΔE , and the spectroscopic factors $(2I+1)S/(2I_{\text{target}}+1)$ are given. The last line states the energy centroid for each spin, the second moment of the distribution as a measure of the width, and the summed strength as the fraction of the sum rule $[2(I+1)/10]$.

j	I	E	ΔE	S	j	I	E	ΔE	S
$s_{1/2}$	4^-	3475	-505	0.004	$d_{5/2}$	6^-	5545	-27	0.948
		3947	-33	0.726			5649	77	0.387
		3996	16	0.042			5572	50	126%
		4262	282	0.060			5490	-28	1.276
		4359	379	0.022			5687	169	0.209
	3912	3980	107	95%			5518	69	114%
$s_{1/2}$	5^-	3198	-662	0.070	$d_{5/2}$	7^-	4038	-1487	0.000
		3708	-152	0.359			4680	-845	0.000
		3961	101	0.475			5086	-439	0.106
		4125	265	0.039			5542	17	1.214
		4180	320	0.013			5695	170	0.149
		4297	437	0.089			5525	131	98%
		3860	249	95%			5317	0	0.515
$d_{3/2}$	3^-	2615	-1490	0.096	$h_{11/2}$	3^+	5317	0	74%
		4051	-54	0.021			4324	-822	0.138
		4255	150	0.370			5217	71	0.231
		4698	593	0.150			5239	93	0.194
	4263	4105	656	91%			5690	544	0.145
$d_{3/2}$	4^-	3475	-775	0.000	$h_{11/2}$	4^+	5146	443	79%
		3947	-303	0.174			5193	0	0.846
		3996	-254	0.000			5193	0	77%
		4262	12	0.680			4424	-605	0.247
		4359	109	0.303			5213	184	0.811
		4711	461	0.024			5029	334	81%
		4250	145	131%			4868	-327	0.000
$d_{3/2}$	5^-	3198	-971	0.000	$h_{11/2}$	7^+	5195	0	1.133
		3708	-461	0.110			5195	0	76%
		3961	-208	0.124			4611	-484	0.229
		4125	-44	0.706			4861	-234	0.284
		4180	11	0.045			5093	-2	0.349
		4297	128	0.331			5340	245	0.445
		4709	540	0.119			5827	732	0.095
				4169			221	131%	
$d_{3/2}$	6^-	3920	-468	0.000	$h_{11/2}$	9^+	5011	-146	0.053
		4206	-182	0.068			5162	5	1.709
		4383	-5	1.240			5157	26	93%
		4481	93	0.193			4895	-337	0.564
		4762	374	0.000			5070	-162	0.564
		4388	51	116%			5537	305	0.289
$d_{5/2}$	4^-	5675	0	0.686			5928	696	0.278
5582	5675	0	76%			5232	377	81%	
$d_{5/2}$	5^-	5482	-90	0.054					

large positive reaction Q value provides this energy, and therefore the reaction is kinematically well matched.

Angular distributions for the $^{208}\text{Pb}(t, \alpha)^{207}\text{Tl}$ reaction at 12 MeV have been measured by Hinds *et al.* [17]. They show negligible cross section at forward angles, a broad maximum around 90° , and a drop by a factor 2 to 180° with little difference for $s_{1/2}$, $d_{3/2}$, $h_{11/2}$, and $d_{5/2}$ pickup. We did a DWBA calculation with the code DWUCK. The calculations predict the same features. As the angular distributions are smooth and very similar for all l values, the measured coincidence rates are proportional to the total cross section. Furthermore the cross section does not change appreciably with α energy over the measured range. Therefore, we can relate the α - γ coincidence rates directly to spectroscopic factors after normalizing at selected states. α - γ coincidence rates, normalized to the spectroscopic factors of Grabmayr *et al.* [6], are shown in Table I, and for comparison the data of Grabmayr *et al.* Our data provide no indication of the transferred angular momentum, and therefore the distinction between $s_{1/2}$ and $d_{3/2}$ transfers, where both are possible for the spin of the state, is taken from [6]. The distinction between $d_{3/2}$ and $d_{5/2}$ is arbitrary; below 4.8 MeV we assume $d_{3/2}$ and above 4.8 MeV $d_{5/2}$ is assumed. This is well justified, because configuration mixing is small. The agreement between the two measurements is quite good, usually within 20%. Larger discrepancies are mostly due to a redistribution of strength between closely spaced levels, unresolved in the $(d, ^3\text{He})$ experiment. Examples for this are the 5086, 5093 keV doublet or the 5537, 5543, 5545 keV triplet. The summed strengths of the multiplets agree in these cases. The errors of the spectroscopic factors cannot be precisely calculated. No errors are given for the spectroscopic factors in [6], on which our calibration is based. The angular distribution of γ rays introduces a systematic error in our data; this is, in general, below 5%. However, for extreme cases as the $10^+ \rightarrow 10^+$ $M1$ transitions, the countrate at 90° might be too small by at most 20% compared to the average over all angles. The total systematic error is estimated as 20%, while the statistical errors of our data can be inferred from Table V. Small γ branches below our experimental sensitivity might contribute to the uncertainty.

Table II summarizes the spectroscopic factors in a physically meaningful way. It is very satisfying that now, after both reassigning some spins (see Sec. IV) and resolving multiplets, the summed strengths are always within 30% of theory. For $s_{1/2}$ and $h_{11/2}$ pickup the agreement is nearly perfect, if one renormalizes the $h_{11/2}$ strength by +25%. For $d_{3/2}$ the summed strengths are always about 25% too high, with the exception of the 3^- levels, the 3^- levels are however highly mixed and some strength might have been missed in the experiment. Only the missing strength in $d_{5/2}$ pick up to 4^- states is then unexplained.

A comparison of the centroids with the unperturbed particle-hole energies, that are however corrected by -300 keV for the Coulomb pairing energy, shows differences below 100 keV, only the 6^+ and 8^+ states of the $h_{9/2}h_{11/2}^{-1}$ deviate by around 200 keV. Therefore the residual interaction is weak, except for the common Coulomb energy. Configuration mixing is stronger for states of natural parity, as is

evident from the width of the strength distribution. For unnatural parity, one level contains the whole strength (or at least 70% of it).

III. THE $^{207}\text{Pb}(d, p)^{208}\text{Pb}$ EXPERIMENT

A. Design of the experiment and procedures

A second possibility to populate states of ^{208}Pb by single-particle transfer, besides the previously discussed proton pickup from ^{209}Bi , is the neutron transfer to ^{207}Pb by the (d, p) reaction. In the model that the ground state of ^{207}Pb consists of a neutron hole in the $p_{1/2}$ orbital, the reaction populates exclusively neutron particle-hole states with the hole in the $p_{1/2}$ orbital and the particle in the lowest orbitals, namely $g_{9/2}$, $i_{11/2}$, $j_{15/2}$, $d_{5/2}$, $s_{1/2}$, $g_{7/2}$, and $d_{3/2}$. The aim is again to study the γ decay of the populated states, and to determine spectroscopic factors with the high resolution that our technique of particle- γ coincidences provides.

The deuteron energy was chosen as 10.0 MeV, just below the Coulomb barrier. At higher energies the γ yield from the $(d, 2n)$ reaction is too strong. Protons are emitted preferentially at backward angles at this bombarding energy, and the experimental setup was therefore similar to that of the $(t, \alpha\gamma)$ study.

The experiment was performed at the tandem accelerator of the Lawrence Livermore National Laboratory. The 10.0 MeV deuteron beam of ~ 7 nA struck a 1 mg/cm^2 metallic ^{207}Pb target (93.2% ^{207}Pb , 5.4% ^{208}Pb , 1.4% ^{206}Pb). The beam was stopped in a shielded Faraday cup 2 m behind the target. Four trapezoidal-shaped Si-detector telescopes were arranged about 2 cm from the target. They covered the angular range between 136° and 151° . The ΔE detectors were $200 \mu\text{m}$ thick and the E detectors consisted of two stacked and electrically connected $500 \mu\text{m}$ detectors. The average energy resolution of the telescopes during the actual experiment was 107 keV. Target and Si detectors were mounted in a stainless steel chamber with 1 mm wall thickness and a diameter of 12 cm. Right outside of this chamber 3 HP-Ge detectors with efficiencies of 10, 20, and 80 % were arranged at 90° ; copper absorbers of 0.1, 1.0, and 3.0 mm thickness, respectively, reduced the countrates of x rays. Approximately 10^8 particle- γ coincidences were registered. The energies deposited in the ΔE , E , and Ge detectors and the times between protons and γ -rays were measured and stored event by event.

Protons were identified by their $\Delta E/E$ ratio in the off line analysis. Deuterons were completely eliminated in this way; for instance, no trace of inelastically scattered deuterons was visible in the proton spectrum coincident with the 570 keV γ line from the first-excited state in ^{207}Pb . The proton energies were internally calibrated from known states in ^{208}Pb . The Ge detectors were calibrated with sources of ^{133}Ba , ^{152}Eu , and $^{56,60}\text{Co}$ below 3.5 MeV. Ground state transitions from states in ^{208}Pb with precisely known energies from a cascade decay of lower-energy lines were used for the energy calibration between 3.5 and 5 MeV. The calibration was extended to the highest measured energy of 7.4 MeV by using single- and double-escape peaks in the previously calibrated region. However, the efficiency of the Ge detectors was not determined experimentally above 3.5 MeV. Below 3.5 MeV,

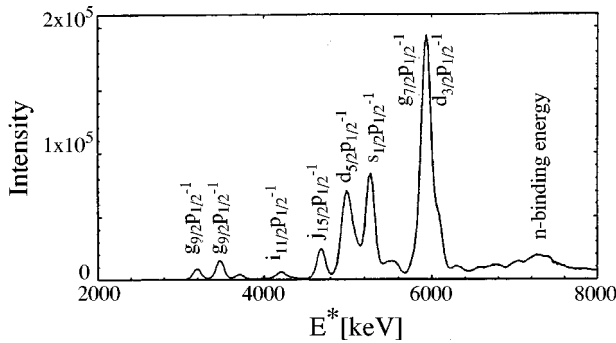


FIG. 3. Proton spectrum in coincidence with all γ rays detected in the 80% Ge detector from $^{207}\text{Pb}(d,p\gamma)^{208}\text{Pb}$. The abscissa gives the corresponding excitation energy in ^{208}Pb .

the efficiency of the 80% detector falls off exponentially with energy. Monte Carlo calculations for comparable detectors show that this dependence continues at higher energies. Therefore the efficiency curve was extrapolated exponentially with an assumed uncertainty that rises to 50% at $E_\gamma = 7$ MeV.

B. Data evaluation and construction of the level scheme

Figure 3 shows the energy spectrum of protons in coincidence with all γ rays. There is a clear structure corresponding to the multiplets of states belonging to one configuration. (The peak of the $j_{15/2}p_{1/2}^{-1}$ configuration is exaggerated by other unresolved states.) The detailed analysis of the data consisted in the iterative examination of γ spectra in coincidence with protons in a narrow energy interval and proton spectra in coincidence with specific γ lines. The analysis proceeded from the low lying states upwards, always using the established γ -decay properties of the lower states populated in the decay of the state of interest. Our technique included generating artificial γ spectra including all the branches from states populated in the primary γ decay. Comparison with the measured spectra showed, for instance in Fig. 4, contaminant lines from $^{208}\text{Pb}(d,p)^{209}\text{Pb}$.

C. Evaluation of spectroscopic factors

Spectroscopic factors can be calculated from the measured population of the levels, provided their spins and parities and the j of the transferred neutron are known. Often only one value of j is possible for a given spin and parity, as $s_{1/2}$ for 0^- , $d_{3/2}$ or $d_{5/2}$ for 2^- , $g_{9/2}$ or $g_{7/2}$ for 4^- , $i_{11/2}$ for 6^- , and $j_{15/2}$ for 7^+ and 8^+ . The spin orbit splitting between $g_{9/2}$ and $g_{7/2}$ is 2.5 MeV and 1 MeV between $d_{5/2}$ and $d_{3/2}$, and configuration mixing is rather weak. Therefore the assumption is justified, that only $j=l+1/2$ is important below

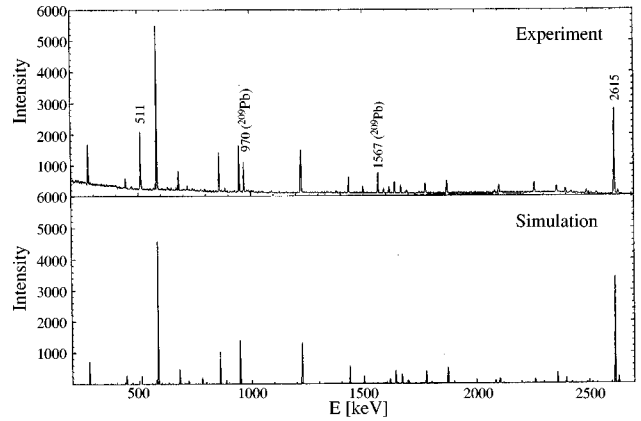


FIG. 4. Measured and simulated (see text) spectrum of the 80% Ge detector in coincidence with protons corresponding to an excitation energy between 5900 and 5960 keV.

5.5 MeV and $j=l-1/2$ above. For the 1^- , 3^- , and 5^- levels the transferred l , as determined from the angular distributions in (d,p) reactions [1] was used.

To extract spectroscopic factors from the measured population of the states the DWBA cross sections have been calculated with the program PTOLEMY [19]. Optical potentials as given in Table III were taken from [20,21]. The results are presented in Table IV and compared with the spectroscopic factors from (d,p) measurements [1]. The spectroscopic factors for the unnatural parity states have been normalized so that the sum for the low lying 4^- states equals 1. This works quite well for the high l values 6 and 7. But for $l=0,2$ only half the expected strength is seen. It is not likely that a significant part of the strength has been missed in the experiment. It is more likely that the DWBA calculations are the source of this discrepancy. The strength for unnatural parity states is always concentrated in only 1 or 2 levels and hard to miss. Very large radii contribute significantly to the cross section, because the neutrons are weakly bound and the deuteron energy is below the Coulomb barrier. The (d,p) measurements at higher deuteron energy also give roughly twice as big spectroscopic factors as deduced here. We assume that all the strength has been found for the unnatural parity states and therefore renormalize the spectroscopic factors for the natural parity states accordingly. This means the spectroscopic factors for natural parity states, as deduced from the comparison with the DWBA calculations, are divided by the sum of the spectroscopic factors of the unnatural parity levels with the same transferred j . An important uncertainty is, that the angular distribution of γ rays is not known. We estimate an error of around 10% for this.

TABLE III. Optical potentials for the DWBA calculations of $^{207}\text{Pb}(d,p)^{208}\text{Pb}$. The real potentials and that of the bound state are of Woods-Saxon type, the imaginary of differentiated Woods-Saxon. Potentials in MeV, radii, and diffuseness a in fm.

	Real			Imaginary		
	V	r_0	a	W	r_0	a
d	116.305	1.25	0.811	13.28	1.40	0.795
p	61.30	1.17	0.750	12.00	1.32	0.658
Bound state			$r_0 = 1.25, RC0 = 1.25, a = 0.65$			

TABLE IV. Spectroscopic factors from $^{207}\text{Pb}(d,p\gamma)^{208}\text{Pb}$. The spectroscopic factors S , not $(2I+1)S$, are listed and compared with those from (d,p) measurements [1]. Some spin assignments are not completely certain; the relevant information on spins is in Table V. See text for the normalization.

E^*	$S_{(d,p\gamma)}$	$S_{(d,p)}$	E^*	$S_{(d,p\gamma)}$	$S_{(d,p)}$
	$l=4$			$j=g_{9/2}$	
	$I^\pi=4^-$			$I^\pi=5^-$	
3475.1	0.972(114)	0.91	3197.7	0.894(112)	0.82
3946.6	0.003(001)	0.00	3708.5	0.212(025)	0.16
3995.6	0.013(003)	$l=(6)$	3961.1	0.000(000)	0.00
4262.0	0.002(001)	0.00	4125.4 ^a	0.014(006)	0.03
4358.8	0.010(001)	0.04	4296.7	0.003(001)	0.02
	$\Sigma = 1.00, E_{\text{av}} = 3493$			$\Sigma = 1.123, E_{\text{av}} = 3312$	
	$l=6$			$j=i_{11/2}$	
	$I^\pi=6^-$			$I^\pi=5^-$	
4206.2	0.810(050)	0.83	4125.4 ^a	0.350(150)	0.12
4383.2	0.022(004)	0.00	4180.2	0.347(044)	0.49
4480.8	0.000(000)	0.00			
5490.3	0.064(004)	0.00			
	$\Sigma = 0.896, E_{\text{av}} = 4302$			$\Sigma = 0.697, E_{\text{av}} = 4153$	
	$l=7$			$j=j_{15/2}$	
	$I^\pi=7^+$			$I^\pi=8^+$	
4867.8	0.866(111)	0.80 ^b	4610.8	0.421(057)	0.39
			4860.8	0.223(034)	^b
			5093.1	0.000(000)	0.00
	$\Sigma = 0.866, E_{\text{av}} = 4868$			$\Sigma = 0.644, E_{\text{av}} = 4697$	
	$l=2$			$j=d_{5/2}$	
	$I^\pi=2^-$			$I^\pi=3^-$	
4229.6	0.031(004)	$l=4$	4051.2	0.003(001)	$l=(6)$
5037.5	0.354(036)	0.52	4254.9	0.010(001)	0.01
5127.4	0.171(015)	0.31	4698.4	0.267(015)	0.23
			4937.5	0.006(002)	0.00
			4953.3	0.000(000)	0.00
			4974.0	0.342(021)	0.43
			5245.3	0.162(004)	0.27
	$\Sigma = 0.556, E_{\text{av}} = 5020$			$\Sigma = 0.790, E_{\text{av}} = 4923$	
	$l=0$			$j=s_{1/2}$	
	$I^\pi=0^-$			$I^\pi=1^-$	
5280.3	0.377(032)	0.99 ^c	4841.4	0.011(004)	0.00
5599.4	0.060(006)	0.10	5292.0	1.071(325)	0.77 ^c
	$\Sigma = 0.437, E_{\text{av}} = 5324$		5512.1	0.074(022)	0.00
	$l=2$			$j=d_{3/2}$	
	$I^\pi=2^-$			$I^\pi=1^-$	
5384.8	0.020(002)	0.05	5947.5	1.266(488)	0.87
5548.1	0.010(001)	0.02	6263.4	0.055(023)	0.04
5923.7	0.349(018)	0.76	6313.7	0.088(038)	0.07
6086.7	0.139(007)	0.27	6360.4	0.029(013)	0.00
			7020.3	0.020(003)	0.06
			7063.4	0.019(010)	0.04
	$\Sigma = 0.518, E_{\text{av}} = 5939$			$\Sigma = 1.477, E_{\text{av}} = 6018$	
	$l=4$			$j=g_{7/2}$	
	$I^\pi=4^-$			$I^\pi=3^-$	
5563.6	0.062(008)	0.07	5347.1	0.033(005)	0.05
5968.6	0.612(053)	1.03	5516.6	0.005(003)	0.07
			5777.9	0.230(023)	0.10
			5813.2	0.077(008)	0.15
			5873.6	0.438(048)	0.57
			6009.6	0.259(027)	0.33
	$\Sigma = 0.673, E_{\text{av}} = 5931$			$\Sigma = 1.042, E_{\text{av}} = 5668$	

^aThe fractions of $l=4$ and $l=6$ are not well determined.

^bThis is the sum for the unresolved 4860.8 and 4867.8 keV states.

^cThe doublet 5280.3 and 5292.0 keV is not resolved in (d,p) .

Table IV shows good agreement with the sum rule strength for $g_{9/2}$ transfer to 5^- states. This is as expected as the normalization was done on the 4^- levels with the same transferred particle; also these states are at low excitation energy. For $i_{11/2}$ transfer, 90% of the sum rule strength is found for the 6^- levels. As the reaction cross section is appreciably lower for $l=6$ transfer than for $l=4$, it is likely that some $l=6$ strength to 5^- states is obscured by simultaneous $g_{9/2}$ transfer. For $j_{15/2}$, nearly the full strength is seen in just one state. Transfer with $l=7$ is very weak for $E_d=10$ MeV and for the mixed 8^+ states some small components might not have been detected in our experiment. As already stated above, it is most likely a shortcoming of the DWBA analysis that the strength to unnatural parity levels of the higher lying configurations is too small by about a factor 2. The 1^- states decay by high-energy $E1$ transitions, for which the γ efficiency is not so certain. Within errors the summed strengths for $s_{1/2}$ and $d_{3/2}$ transfer agree with the sum rule. It is also possible that some strength should be redistributed between $s_{1/2}$ and $d_{3/2}$; for this we have to rely completely on the (d,p) results.

Some aspects of individual states have been clarified. Level spins determined from the γ decay have ruled out wrong l assignments for the states at 3995, 4051, and 4230 keV. Resolved doublets include the 7^+ , 8^+ at 4868 and 4861 keV, the 0^- , 1^- states at 5280 and 5292 keV, and the 1^- , 3^- doublet at 5512, 5516 keV.

IV. THE LEVEL SCHEME

Our summary of the level scheme and the γ transitions of ^{208}Pb is presented in Table V. All measured γ energies have been used in a least squares fit to determine optimized level energies and their errors; the recoil energy of the γ quanta has not been taken into account. Spin and parity assignments are based primarily on the γ decay, the transferred l and spectroscopic factors of the transfer reactions and previous data, mainly as compiled by Martin [1]. $M1$ transitions dominate the γ decay in general. $E2$ transitions compete only if the structure of the levels is very favorable. Low-energy (≤ 1 MeV) $E1$ transitions are slow.

Figure 5, originally due to Jan Blomqvist [26] and updated with the present data, is used as a guideline. It shows all states that are expected from single-particle–single-hole excitations and the few two-particle–two-hole states that are low enough in energy due to their special structure. The configuration assignments in this figure classify the states. The real levels are of course often of mixed configurations.

Up to level 25 of Table V (the 8^+ state at 4611 keV) all expected levels are now identified experimentally with definite assignments of spin and parity. The (7^-) level nr 26 is based only on a γ transition observed in $(n,n'\gamma)$ [7]. The spin assignments to levels 28–30 are not completely certain from experiment alone, but if there is only one 4^- , 5^- , and 6^- state here as predicted by the shell model, then assignments can be made. Level 32 is only seen in $(d,p\gamma)$ with very weak intensity and therefore questionable. The states at 4861 and 4868 keV belong to the $\nu j_{15/2}p_{1/2}^{-1}$ configuration and had been an unresolved doublet so far. States 37 to 39 have been assigned 3^- by Martin [1]. This is compatible with the present data and strictly proven for the 4974 keV

level. The γ decay of level 44 strongly favors the (7^-) assignment over the also possible values 5^- , 6^- , if one considers its structure [14]. Five states, namely 27, 39, 41, 46, and 56, are strongly populated by transfer of a $d_{5/2}$ neutron to ^{207}Pb . Spin and parity 2^- is excluded for the levels 27, 39, and 56 from their γ decay. A 2^- assignment for level 41 and 46 is suggested from their γ decay and it is favored, to obtain a physically possible distribution of the $d_{5/2}$ transfer strength. No configurations exist to which $M1$ transitions from $\nu d_{5/2}p_{1/2}^{-1}$ are allowed. On the other hand, strong $E2$ transitions, preferentially with $\Delta I=+2$, can populate the states of the $\nu g_{9/2}p_{1/2}^{-1}$ configuration and are indeed seen. The $(t,\alpha\gamma)$ and the $(d,p\gamma)$ measurements both give a level at 5317 keV (60,61), but with different γ decays. We conclude therefore that there are two states. For level 60, a 3^+ assignment agrees with its γ decay and gives the correct strength for the $h_{11/2}$ proton pickup; configuration mixing is likely negligible for this state of unnatural parity as is also found for the 5^+ and 7^+ levels (49,50).

Most of the levels from 72 to 83 are populated by $l=2$ proton pickup and have therefore a $\pi h_{9/2}d_{5/2}^{-1}$ component. States with spin 2^- and 3^- might decay directly to the ground state via high-energy γ rays out of the measuring range ($E_\gamma \leq 4$ MeV) of the $(t,\alpha\gamma)$ experiment. This might explain the poor correspondence of the levels with those seen in $(d,^3\text{He})$. Also there is too little pickup strength found for the 4^- states; perhaps one of the levels with a tentative (5^-) assignment (e.g., 79) is instead 4^- .

At still higher energies the increased level density prohibits in general a detailed discussion of the states. A clear picture emerges only for the near yrast states, as discussed in [8]. The second 11^+ state from the work of Broda *et al.* [25] has been added in Table V. The excitation energies of both 11^+ states established from the measurement of γ transitions disagree with the results from inelastic electron scattering [5].

The (d,p) reaction populates the states of the $\nu d_{3/2}p_{1/2}^{-1}$ and $\nu g_{7/2}p_{1/2}^{-1}$ configuration at about 6 MeV. If the angular distribution of the (d,p) measurements [1] establishes $l=2$, the γ decay distinguishes clearly between 1^- and 2^- states; for $l=1^-$, a ground state γ transition is expected, while for 2^- , a branching to other states is anticipated (an $M2$ decay to the ground state cannot be excluded). In this way levels 95 and 104 are assigned 2^- . Then the spectroscopic factors from (d,p) agree with the sum rule, and those extracted from the present experiment are lower by a factor 2 than the (d,p) results for all 2^- states. The 1^- assignments are definite for levels 97, 111, 113, and 119 in agreement with (γ,γ') results [1].

The strongest state in $l=4$ transfer is at 5968 keV (level 99). The γ branch to a 6^- level gives this level spin as 4^- . This is again a favored $E2$ transition from $g_{7/2}p_{1/2}^{-1}$ to $i_{11/2}p_{1/2}^{-1}$ with $\Delta I=2$. In the (d,p) measurements, this level exhausts the sum rule. Therefore the other strongly populated levels 86, 93, and 102 are assigned as 3^- states; the γ decay of level 86 and 102 also rules out spin parity 4^- definitively.

V. CONCLUSIONS

The present study has found many new γ transitions in ^{208}Pb , resolved previously unrecognized multiplets, revised

TABLE V. Levels and γ transitions in ^{208}Pb . The columns show (2) level energies and errors from a least squares fit of all measured γ energies; (3) assigned spins; (4) measured energies of depopulating γ rays and their errors; (5) measured γ -branching ratios of the transitions and their errors; (6) and (7) energies and spins of the populated states; (8) the first number gives the relative population strength in (d,p), the second number in *italic* gives the population strength in (t,α), it is the actually measured number of α - γ coincidences divided by 100. The population strengths take into account electron conversion, if necessary, and additional γ decays, seen only in the other experiment. Additional high-energy transitions from Radermacher *et al.* are marked by [10]; the population strength is not corrected for these additional decays. The error of the strength of the (dp) measurement is statistical only. The additional systematic error due to angular distributions and γ efficiency is 10% below 3.5 MeV and rises to 50% at 7 MeV (see text). See also the footnotes for individual states; footnotes are labeled by level numbers.

No.	$E_{\text{ini}}^{\text{level}}$ (keV)	I_{ini}^{π} (\hbar)	E_{γ} (keV)	I_{γ} (%)	$E_{\text{fin}}^{\text{level}}$ (keV)	I_{fin}^{π} (\hbar)	S_{expt} Relative
1		0^{+}			Ground state		
2	2614.549(13)	3^{-}	2614.55(1)	100.00	Ground state	0^{+}	1.41(0.29) <i>1.41(0.21)</i>
3	3197.740(13)	5^{-}	583.19(1)	100.00	2614.549(13)	3^{-}	70.41(2.20) <i>1.60(0.16)</i>
4	3475.103(15)	4^{-}	277.35(1)	34.68(1.32)	3197.740(13)	5^{-}	70.34(1.72)
			860.56(1)	65.32(2.06)	2614.549(13)	3^{-}	<i>0.09(0.05)</i>
5	3708.511(43)	5^{-}	233.12(30)	1.84(0.57)	3475.103(15)	4^{-}	20.89(1.02)
			510.70(7)	95.19(4.76)	3197.740(13)	5^{-}	<i>9.83(0.80)</i>
			1093.96(24)	2.97(0.85)	2614.549(13)	3^{-}	
6	3919.987(70)	6^{-}	211.45(20)	44.85(4.12)	3708.511(43)	5^{-}	
			722.22(10)	55.15(6.19)	3197.740(13)	5^{-}	
7	3946.620(100)	4^{-}	238.13(15)	16.68(1.18)	3708.511(43)	5^{-}	0.23(0.01)
			471.60(35)	17.36(1.24)	3475.103(15)	4^{-}	<i>19.15(1.40)</i>
			748.94(15)	65.96(4.60)	3197.740(13)	5^{-}	
8	3961.138(46)	5^{-}	252.58(10)	29.80(2.06)	3708.511(43)	5^{-}	
			486.0(10)	1.57(0.59)	3475.103(15)	4^{-}	<i>12.68(1.00)</i>
			763.40(5)	68.63(4.80)	3197.740(13)	5^{-}	
9	3995.585(60)	4^{-}	797.92(11)	18.09(4.26)	3197.740(13)	5^{-}	1.18(0.24)
			1381.00(8)	81.91(20.21)	2614.549(13)	3^{-}	<i>0.95(0.25)</i>
10	4037.514(75)	7^{-}	117.50(20)	11.58(4.21)	3919.987(70)	6^{-}	
			839.75(10)	88.42(13.68)	3197.740(13)	5^{-}	
11	4051.194(40)	3^{-}	576.06(10)	15.51(1.46)	3475.103(15)	4^{-}	0.57(0.03)
			1436.65(5)	84.49(4.75)	2614.549(13)	3^{-}	<i>0.26(0.08)</i>
12	4085.450(150)	2^{+}	4085.40(30)	100.00	ground state	0^{+}	
13	4125.444(44)	5^{-}	164.34(20)	3.74(0.51)	3961.138(46)	5^{-}	2.27(0.21)
			179.50(60)	0.71(0.20)	3946.620(100)	4^{-}	<i>11.25(0.90)</i>
			416.89(20)	3.74(0.81)	3708.511(43)	5^{-}	
			650.30(10)	14.75(3.03)	3475.103(15)	4^{-}	
			927.70(5)	77.07(9.29)	3197.740(13)	5^{-}	
14	4180.200(100)	5^{-}	705.19(23)	16.20(4.23)	3475.103(15)	4^{-}	2.46(0.23)
			982.44(11)	83.80(8.45)	3197.740(13)	5^{-}	<i>0.85(0.15)</i>
15	4206.200(90)	6^{-}	498.03(25)	17.82(2.34)	3708.511(43)	5^{-}	7.67(0.47)
			1008.38(10)	82.18(5.74)	3197.740(13)	5^{-}	<i>0.99(0.20)</i>
16	4229.620(50)	2^{-}	1615.00(10)	88.63(8.90)	2614.549(13)	3^{-}	7.62(0.72)
			4229.50(30)	11.37(3.04)	Ground state	0^{+}	
17	4254.880(50)	3^{-}	779.20(40)	3.82(0.96)	3475.103(15)	4^{-}	1.50(0.10)
			1640.32(15)	96.18(6.75)	2614.549(13)	3^{-}	<i>6.60(0.15)</i>
18	4262.000(55)	4^{-}	553.50(10)	22.41(1.84)	3708.511(43)	5^{-}	0.17(0.01)
			786.85(10)	27.00(2.20)	3475.103(15)	4^{-}	<i>11.24(0.90)</i>
			1064.36(20)	2.11(0.28)	3197.740(13)	5^{-}	
			1647.47(20)	48.48(3.86)	2614.549(13)	3^{-}	
19	4296.700(80)	5^{-}	171.00(20)	3.09(0.81)	4125.444(44)	5^{-}	0.42(0.03)
			588.18(30)	58.37(5.85)	3708.511(43)	5^{-}	<i>6.89(0.70)</i>
			821.60(10)	33.33(3.41)	3475.103(15)	4^{-}	
			1099.10(30)	5.20(1.63)	3197.740(13)	5^{-}	

TABLE V. (Continued).

No.	$E_{\text{ini}}^{\text{level}}$ (keV)	I_{ini}^{π} (\hbar)	E_{γ} (keV)	I_{γ} (%)	$E_{\text{fin}}^{\text{level}}$ (keV)	I_{fin}^{π} (\hbar)	S_{expt} Relative
20	4323.930(130)	4 ⁺	362.50(50)	11.84(5.26)	3961.138(46)	5 ⁻	0.09(0.02)
			1126.30(20)	88.16(27.63)	3197.740(13)	5 ⁻	0.79(0.18)
21	4358.785(63)	4 ⁻	178.50(50)	1.28(0.64)	4180.200(100)	5 ⁻	1.10(0.08)
			362.75(50)	1.70(0.43)	3995.585(60)	4 ⁻	0.43(0.50)
			883.65(8)	61.49(5.53)	3475.103(15)	4 ⁻	
			1161.10(10)	23.83(3.62)	3197.740(13)	5 ⁻	
			1744.30(40)	11.70(1.70)	2614.549(13)	3 ⁻	
22	4383.246(65)	6 ⁻	176.80(50)	0.80(0.23)	4206.200(90)	6 ⁻	0.23(0.04)
			257.70(50)	0.63(0.23)	4125.444(44)	5 ⁻	18.21(1.30)
			463.20(10)	4.79(0.74)	3919.987(70)	6 ⁻	
			1185.54(8)	93.79(17.84)	3197.740(13)	5 ⁻	
23	4423.630(75)	6 ⁺	715.20(30)	9.09(2.27)	3708.511(43)	5 ⁻	0.13(0.04)
			1225.85(10)	90.91(28.41)	3197.740(13)	5 ⁻	1.28(0.20)
24	4480.750(100)	6 ⁻	771.60(40)	6.05(2.49)	3708.511(43)	5 ⁻	
			1283.00(10)	93.95(8.54)	3197.740(13)	5 ⁻	2.84(0.27)
25	4610.795(70)	8 ⁺	573.80(50)	3.19(0.80)	4037.514(75)	7 ⁻	2.12(0.19)
			1413.16(10)	96.81(9.16)	3197.740(13)	5 ⁻	1.31(0.20)
26?	4680.310(250)	(7 ⁻)	760.32(25)	100.00	3919.987(70)	6 ⁻	
27	4698.375(40)	3 ⁻	436.31(9)	3.56(0.32)	4262.000(55)	4 ⁻	65.18(1.77)
			443.57(8)	16.85(0.82)	4254.880(50)	3 ⁻	1.99(0.40)
			468.76(7)	4.08(0.36)	4229.620(50)	2 ⁻	
			612.88(15)	0.69(0.22)	4085.450(150)	2 ⁺	
			647.28(17)	1.75(0.35)	4051.194(40)	3 ⁻	
			702.86(14)	1.68(0.25)	3995.585(60)	4 ⁻	
			1223.30(5)	40.94(1.97)	3475.103(15)	4 ⁻	
			1500.44(13)	17.71(1.07)	3197.740(13)	5 ⁻	
			2083.78(11)	11.16(1.19)	2614.549(13)	3 ⁻	
			4699.35(80)	1.58(0.19)	Ground state	0 ⁺	
28	4709.490(250)	(5 ⁻)	413.0(10)	5.33(2.96)	4296.700(80)	5 ⁻	
			714.0(10)	4.73(2.37)	3995.585(60)	4 ⁻	1.75(0.30)
			748.30(50)	28.99(4.14)	3961.138(46)	5 ⁻	
			1000.76(40)	39.64(5.92)	3708.511(43)	5 ⁻	
			1511.90(40)	21.30(4.14)	3197.740(13)	5 ⁻	
29	4711.300(750)	(4 ⁻)	1236.0(10)	27.78(2.78)	3475.103(15)	4 ⁻	
			2096.9(10)	72.22(19.44)	2614.549(13)	3 ⁻	0.36(0.12)
30	4761.800(250)	(6 ⁻)	1564.07(25)	100.00	3197.740(13)	5 ⁻	
31	4841.400(100)	1 ⁻	4841.24(35)	100.00	Ground state	0 ⁺	2.01(0.40)
32?	4857.500(350)		772.00(30)	100.00	4085.450(150)	2 ⁺	0.21(0.10)
33	4860.840(80)	8 ⁺	250.04(5)	74.04(7.69)	4610.795(70)	8 ⁺	1.14(0.11)
			823.30(20)	25.96(4.81)	4037.514(75)	7 ⁻	1.62(0.16)
34	4866.00(200)	0 ⁺		No γ transition known			
35	4867.816(80)	7 ⁺	257.09(9)	30.79(4.58)	4610.795(70)	8 ⁺	4.57(0.49)
			386.71(30)	19.59(6.87)	4480.750(100)	6 ⁻	
			444.15(10)	29.52(5.85)	4423.630(75)	6 ⁺	
			484.65(30)	9.67(3.56)	4383.246(65)	6 ⁻	
			830.00(40)	10.43(3.56)	4037.514(75)	7 ⁻	
36	4895.277(80)	10 ⁺	34.50(30)	0.03(0.01)	4860.840(80)	8 ⁺	
			284.48(5)	83.80(7.35)	4610.795(70)	8 ⁺	3.32(0.30)
			857.72(10)	16.17(2.94)	4037.514(75)	7 ⁻	
37	4937.550(200)	3 ⁻	2323.50(60)	100.00	2614.549(13)	3 ⁻	1.60(0.42)
							1.21(0.20)
			4934.7(1)	7(1)	Ground state	0 ⁺	[10]
38	4953.320(230)	3 ⁻	2338.77(23)	100.00	2614.549(13)	3 ⁻	

TABLE V. (Continued).

No.	$E_{\text{ini}}^{\text{level}}$ (keV)	I_{ini}^{π} (\hbar)	E_{γ} (keV)	I_{γ} (%)	$E_{\text{fin}}^{\text{level}}$ (keV)	I_{fin}^{π} (\hbar)	S_{expt} Relative
39	4974.037(40)	3^{-}	275.72(24)	0.58(0.23)	4698.375(40)	3^{-}	96.82(2.14)
			615.68(45)	0.64(0.21)	4358.785(63)	4^{-}	
			712.13(25)	1.16(0.22)	4262.000(55)	4^{-}	
			719.11(7)	6.99(0.42)	4254.880(50)	3^{-}	
			1265.00(60)	1.29(0.45)	3708.511(43)	5^{-}	
			1499.03(10)	7.95(0.52)	3475.103(15)	4^{-}	
			1776.20(15)	39.92(1.44)	3197.740(13)	5^{-}	
			2359.48(6)	40.55(1.38)	2614.549(13)	3^{-}	
40	5010.550(90)	9^{+}	4974.00(80)	0.92(0.26)	Ground state	0^{+}	$0.30(0.10)$
			115.20(20)	3.61(1.03)	4895.277(80)	10^{+}	
41	5037.520(50)	$2^{-}(3^{-})$	399.75(5)	96.39(6.70)	4610.795(70)	8^{+}	132.81(7.59)
			807.90(9)	3.85(0.36)	4229.620(50)	2^{-}	
42	5069.380(130)	10^{+}	986.37(10)	3.26(0.21)	4051.194(40)	3^{-}	$3.22(0.30)$
			1562.34(10)	6.37(0.44)	3475.103(15)	4^{-}	
			2423.02(8)	85.38(5.69)	2614.549(13)	3^{-}	
			5037.47(60)	1.15(0.15)	Ground state	0^{+}	
			174.10(10)	100.00	4895.277(80)	10^{+}	
43	5075.800(200)	1367.0(10)	100.00	3708.511(43)	5^{-}	$0.15(0.07)$	
44	5085.550(250)	(7^{-})	702.1(10)	11.19(3.73)	4383.246(65)	6^{-}	$1.38(0.15)$
			879.30(30)	88.81(9.70)	4206.200(90)	6^{-}	
45	5093.110(200)	8^{+}	232.20(30)	6.51(2.37)	4860.840(80)	8^{+}	$1.99(0.20)$
			482.35(20)	93.49(8.28)	4610.795(70)	8^{+}	
46	5127.420(90)	$2^{-},(3^{-})$	1652.20(17)	5.81(0.65)	3475.103(15)	4^{-}	67.10(2.16)
			2513.00(10)	87.63(3.08)	2614.549(13)	3^{-}	
			5126.75(70)	6.57(0.66)	Ground state	0^{+}	
			2520.17(45)	100.00	2614.549(13)	3^{-}	
47?	5134.720(450)	9^{+}	266.70(20)	9.04(1.57)	4895.277(80)	10^{+}	1.64(0.29)
			301.25(10)	11.79(1.77)	4860.840(80)	8^{+}	
48	5162.100(90)	9^{+}	551.32(5)	54.03(4.32)	4610.795(70)	8^{+}	$9.76(1.00)$
			769.83(20)	45.20(12.58)	4423.630(75)	6^{+}	
			869.44(20)	44.99(4.48)	4323.930(130)	4^{+}	
49	5193.400(150)	5^{+}	1995.50(50)	9.81(3.84)	3197.740(13)	5^{-}	$4.83(0.70)$
			327.44(20)	14.26(1.68)	4867.816(80)	7^{+}	
50	5195.340(140)	7^{+}	334.50(40)	2.01(0.67)	4860.840(80)	8^{+}	$6.20(1.00)$
			584.4(10)	Questionable	4610.795(70)	8^{+}	
			715.00(60)	1.68(0.17)	4480.750(100)	6^{-}	
			771.74(20)	76.34(10.74)	4423.630(75)	6^{+}	
			1275.50(50)	5.70(2.35)	3919.987(70)	6^{-}	
			789.35(20)	61.15(4.86)	4423.630(75)	6^{+}	
51	5213.000(200)	6^{+}	2015.50(50)	38.85(7.73)	3197.740(13)	5^{-}	$4.63(0.50)$
			892.40(40)	23.66(6.87)	4323.930(130)	4^{+}	
52	5216.540(300)	4^{+}	2602.0(10)	76.34(15.27)	2614.549(13)	3^{-}	$1.32(0.25)$
			340.16(15)	100.00	4895.277(80)	10^{+}	
53	5235.440(180)	11^{+}					
54	5241	0^{+}	2626	100.00	2614.549(13)	3^{-}	
55	5239.350(360)	3^{-}	2625.20(50)	100.00	2614.549(13)	3^{-}	$1.11(0.23)$
56	5245.280(60)	3^{-}	307.80(20)	1.23(0.45)	4937.550(200)	3^{-}	52.71(1.35)
			921.77(40)	1.41(0.40)	4323.930(130)	4^{+}	
			1193.87(35)	1.71(0.57)	4051.194(40)	3^{-}	
			1770.54(35)	5.54(0.94)	3475.103(15)	4^{-}	
			2630.80(10)	90.11(2.20)	2614.549(13)	3^{-}	
			5244.4(10)	2(1)	Ground state	0^{+}	
57	5254.160(150)	3^{-}	178.34(10)	15.72(4.11)	5075.800(200)		[10] $7.72(0.91)$
			1779.06(15)	84.28(9.63)	3475.103(15)	4^{-}	

TABLE V. (Continued).

No.	$E_{\text{ini}}^{\text{level}}$ (keV)	I_{ini}^{π} (\hbar)	E_{γ} (keV)	I_{γ} (%)	$E_{\text{fin}}^{\text{level}}$ (keV)	I_{fin}^{π} (\hbar)	S_{expt} Relative
58	5280.322(80)	0^{-}	438.83(5) 1050.75(8)	21.62(0.99) 78.38(2.22)	4841.400(100) 4229.620(50)	1^{-} 2^{-}	65.29(1.59)
59	5292.000(200)	1^{-}	5291.88(15)	100.00	Ground state	0^{+}	245.24(4.42)
60	5317.000(220)	(3^{+})	993.17(20) 2702.00(50)	79.93(7.96) 20.07(5.19)	4323.930(130) 2614.549(13)	4^{+} 3^{-}	$2.94(0.30)$
61	5317.300(600)		2119.54(60)	100.00	3197.740(13)	5^{-}	0.97(0.26)
62	5339.460(160)	8^{+}	478.70(20) 728.60(20) 1302.0(10)	33.61(4.20) 52.94(5.88) 13.45(3.78)	4860.840(80) 4610.795(70) 4037.514(75)	8^{+} 8^{+} 7^{-}	$2.54(0.30)$
63	5347.150(250)	3^{-}	1295.84(50) 2732.63(25)	15.56(5.76) 84.44(10.66)	4051.194(40) 2614.549(13)	3^{-} 3^{-}	2.96(0.36)
64	5380.650(800)		2766.10(80)	100.00	2614.549(13)	3^{-}	$1.38(0.22)$
65	5383.74(111)		1387.8(10)	100.00	3995.585(60)	4^{-}	$0.50(0.10)$
66	5384.780(100)	$2^{-}(3^{-})$	1155.10(12) 1333.50(22) 2770.49(20) 5384.60(80)	34.25(4.38) 10.09(2.38) 43.86(3.71) 11.80(2.28)	4229.620(50) 4051.194(40) 2614.549(13) Ground state	2^{-} 3^{-} 3^{-} 0^{+}	8.96(0.59)
67	5482.10(100)	5^{-}	2867.5(10)	100.00	2614.549(13)	3^{-}	$0.70(0.20)$
68	5490.320(150)	6^{-}	1107.00(50) 1193.53(20) 1283.5(10) 1365.00(50) 1529.00(50) 1570.80(50) 1781.50(50) 2292.76(25)	15.33(2.44) 10.87(1.65) 6.41(1.22) 18.45(2.38) 13.87(2.38) 7.27(1.59) 12.77(2.69) 15.03(3.48)	4383.246(65) 4296.700(80) 4206.200(90) 4125.444(44) 3961.138(46) 3919.987(70) 3708.511(43) 3197.740(13)	6^{-} 5^{-} 6^{-} 5^{-} 5^{-} 6^{-} 5^{-} 5^{-}	0.87(0.06) $16.50(2.70)$
69	5512.100(300)	1^{-}	5512.06(30)	100.00	Ground state	0^{+}	18.72(1.95)
70	5516.600(350)	3^{-}	2902.30(50)	100.00	2614.549(13)	3^{-}	0.45(0.21)
71	5536.640(200)	10^{+}	467.30(20) 641.26(30)	18.79(4.85) 81.21(9.09)	5069.380(130) 4895.277(80)	10^{+} 10^{+}	$1.65(0.20)$
72	5542.040(180)	7^{-}	457.45(20) 1062.90(50) 1119.1(10) 1159.60(30) 1336.50(50) 1505.90(50) 1623.20(50)	12.29(1.37) 6.93(1.05) 2.94(1.18) 42.68(3.40) 18.30(2.03) 10.78(1.83) 6.08(1.83)	5085.550(250) 4480.750(100) 4423.630(75) 4383.246(65) 4206.200(90) 4037.514(75) 3919.987(70)	7^{-} 6^{-} 6^{+} 6^{-} 6^{-} 7^{-} 6^{-}	$15.72(1.60)$
73	5545.470(110)	5^{-}	1248.50(50) 1283.50(10) 1420.30(50) 1583.80(50) 1599.10(50) 1836.60(50) 2347.0(10)	4.91(0.98) 13.02(2.62) 11.30(2.29) 7.53(2.62) 11.30(1.72) 29.89(3.60) 22.03(4.42)	4296.700(80) 4262.000(55) 4125.444(44) 3961.138(46) 3946.620(100) 3708.511(43) 3197.740(13)	5^{-} 4^{-} 5^{-} 5^{-} 4^{-} 5^{-} 5^{-}	$12.28(2.50)$
74	5548.080(200)		2933.53(20) 5547.9(18)	100.00 2(1)	2614.549(13) Ground state	3^{-} 0^{+}	4.73(0.48) [10]
75	5563.580(140)	$3^{-}, 4^{-}$	2949.03(14)	100.00	2614.549(13)	3^{-}	10.13(0.80)
76	5566.000(600)		2090.3(10)	100.00	3475.103(15)	4^{-}	0.43(0.22)
77	5599.400(80)	0^{-}	757.94(7) 1369.74(7)	33.08(3.35) 66.92(5.81)	4841.400(100) 4229.620(50)	1^{-} 2^{-}	12.26(0.82)
78	5641.100(500)		5641.10(50)	100.00	Ground state	0^{+}	0.61(0.22)

TABLE V. (Continued).

No.	$E_{\text{ini}}^{\text{level}}$ (keV)	I_{ini}^{π} (\hbar)	E_{γ} (keV)	I_{γ} (%)	$E_{\text{fin}}^{\text{level}}$ (keV)	I_{fin}^{π} (\hbar)	S_{expt} Relative
79	5649.700(280)	(5^-)	1387.4(10)	11.60(3.00)	4262.000(55)	4^-	5.02(0.90)
			1523.8(10)	27.20(4.60)	4125.444(44)	5^-	
			1654.20(50)	19.60(4.00)	3995.585(60)	4^-	
			2451.30(80)	33.20(5.00)	3197.740(13)	5^-	
			3034.5(10)	8.40(2.60)	2614.549(13)	3^-	
80	5675.170(270)	(4^-)	1317.0(10)	3.61(1.47)	4358.785(63)	4^-	8.89(1.00)
			1413.0(10)	7.34(1.47)	4262.000(55)	4^-	
			1420.0(10)	15.58(3.16)	4254.880(50)	3^-	
			3060.60(30)	73.48(6.66)	2614.549(13)	3^-	
81	5686.860(600)	6^-	1561.0(10)	33.46(8.55)	4125.444(44)	5^-	2.70(0.70)
			1726.0(10)	35.32(10.78)	3961.138(46)	5^-	
			1767.0(10)	31.23(6.32)	3919.987(70)	6^-	
82	5689.950(300)	4^+	3075.40(30)	100.00	2614.549(13)	3^-	0.83(0.17)
83	5695.100(500)	7^-	1775.10(50)	100.00	3919.987(70)	6^-	1.93(0.30)
84	5715.900(900)	(2^+)	5715.90(90)	100.00	Ground state	0^+	
85	5750	11^+	680.5	80	5069.380(130)	10^+	
			854.7	20	4895.277(80)	10^+	
86	5777.900(120)	3^-	1523.05(15)	12.74(1.57)	4254.880(50)	3^-	20.79(1.35)
			1726.68(17)	11.92(1.82)	4051.194(40)	3^-	1.67(0.27)
			3163.50(30)	71.70(6.00)	2614.549(13)	3^-	
			5777.26(60)	3.64(0.74)	Ground state	0^+	
87	5782.000(600)		1398.78(60)	100.00	4383.246(65)	6^-	0.61(0.19)
88	5799.300(500)		2324.19(50)	100.00	3475.103(15)	4^-	1.41(0.35)
89	5805.900(900)	1	5805.90(90)	100.00	Ground state	0^+	0.45(0.16)
90	5813.210(170)	$3^-(4^-)$	2338.21(26)	45.87(5.92)	3475.103(15)	4^-	7.02(0.57)
			3198.60(21)	54.13(5.55)	2614.549(13)	3^-	
91	5826.190(500)	(8^+)	1215.40(50)	100.00	4610.795(70)	8^+	0.54(0.10)
92	5846.10(110)	1^+	5846.1(11)	100.00	Ground state	0^+	
93	5873.560(140)	3^-	2398.45(10)	100.00	3475.103(15)	4^-	40.55(1.74)
94	5885.240(200)		1588.50(50)	12.57(5.42)	4296.700(80)	5^-	12.52(1.27)
			3270.70(20)	87.43(8.60)	2614.549(13)	3^-	1.10(0.20)
95	5923.734(40)	2^-	631.34(30)	1.03(0.19)	5292.000(200)	1^-	198.10(4.04)
			678.50(8)	8.56(0.33)	5245.280(60)	3^-	
			796.70(35)	1.10(0.19)	5127.420(90)	2^-	
			886.36(25)	2.22(0.25)	5037.520(50)	$2^-, 3^-$	
			949.70(6)	27.90(0.85)	4974.037(40)	3^-	
			1225.42(7)	27.35(1.31)	4698.375(40)	3^-	
			1668.60(20)	7.45(0.44)	4254.880(50)	3^-	
			1694.10(17)	2.98(0.30)	4229.620(50)	2^-	
			1872.46(8)	14.57(0.81)	4051.194(40)	3^-	
			3309.14(21)	3.76(0.50)	2614.549(13)	3^-	
			5922.6(10)	3.09(0.57)	Ground state	0^+	
96	5928.000(300)	10^+	858.40(35)	35.22(12.58)	5069.380(130)	10^+	
			1032.98(40)	64.78(8.18)	4895.277(80)	10^+	1.59(0.16)
97	5947.460(450)	1^-	5947.18(50)	100.00	Ground state	0^+	205.22(15.18)
98	5966.360(230)		749.63(40)	100.00	5216.540(300)	4^+	1.00(0.30)
99	5968.600(60)	4^-	1644.10(80)	0.74(0.35)	4323.930(130)	4^+	110.54(4.42)
			1762.56(30)	2.42(0.23)	4206.200(90)	6^-	
			2260.05(8)	24.68(1.51)	3708.511(43)	5^-	

TABLE V. (Continued).

No.	$E_{\text{ini}}^{\text{level}}$ (keV)	I_{ini}^{π} (\hbar)	E_{γ} (keV)	I_{γ} (%)	$E_{\text{fin}}^{\text{level}}$ (keV)	I_{fin}^{π} (\hbar)	S_{expt} Relative
99	5968.600(60)	4 ⁻	2260.05(8) 2770.92(8)	24.68(1.51) 72.16(3.68)	3708.511(43) 3197.740(13)	5 ⁻ 5 ⁻	
100	5972.870(370)	2 ⁺	1648.50(50)	28.65(10.16)	4323.930(130)	4 ⁺	3.25(0.63)
101	5992.640(260)	6 ⁺	5973.50(80) 779.75(50) 797.40(50)	71.35(16.67) 12.84(5.42) 16.09(5.97)	Ground state 5213.000(200) 5195.340(140)	0 ⁺ 6 ⁺ 7 ⁺	3.00(0.44)
102	6009.630(90)	3 ⁻	1511.60(60) 1609.32(60) 1685.76(35)	19.71(6.15) 21.70(6.87) 9.17(1.38)	4480.750(100) 4383.246(65) 4323.930(130)	6 ⁻ 6 ⁻ 4 ⁺	24.76(1.85)
103	6026.050(600)		1924.22(20) 2534.51(10) 2030.45(60)	20.55(3.00) 70.28(6.72) 100.00	4085.450(150) 3475.103(15) 3995.585(60)	2 ⁺ 4 ⁻ 4 ⁻	1.74(0.46)
104	6086.711(50)	(2) ⁻	841.41(20) 959.53(30) 1112.65(8)	2.17(0.23) 1.05(0.23) 11.90(0.92)	5245.280(60) 5127.420(90) 4974.037(40)	3 ⁻ 2 ⁻ 3 ⁻	84.99(2.46)
			1388.30(7) 1831.87(10) 1857.02(11)	22.86(1.09) 17.28(1.37) 11.95(1.09)	4698.375(40) 4254.880(50) 4229.620(50)	3 ⁻ 3 ⁻ 2 ⁻	
			2035.61(10) 3472.42(35) 6087.5(20)	22.96(1.35) 8.38(1.09) 1.6(3)	4051.194(40) 2614.549(13) Ground state	3 ⁻ 3 ⁻ 0 ⁺	[10]
105	6099.850(370)		860.51(6) 1802.75(50)	68.75(18.75) 31.25(12.50)	5239.350(360) 4296.700(80)	5 ⁻	2.78(0.63)
106	6100.790(270)	12 ⁺	351.4 865.35(20)	20 80	5750 5235.440(180)	11 ⁺ 11 ⁺	
107	6104.100(550)		538.00(40) 1807.60(60)	61.22(15.31) 38.78(17.86)	5566.000(600) 4296.700(80)	5 ⁻	1.68(0.39)
108	6147.850(800)		2672.75(80)	100.00	3475.103(15)	4 ⁻	0.67(0.15)
109	6242.450(900)		3627.90(90)	100.00	2614.549(13)	3 ⁻	0.50(0.17)
110	6250.50(500)		3636.0(50)	100.00	2614.549(13)	3 ⁻	0.50(0.15)
111	6263.400(300)	1 ⁻	6263.40(30)	100.00	Ground state	0 ⁺	10.29(0.76)
112	6274.350(260)	3 ⁻	757.78(35) 2278.34(45) 3659.75(35)	12.50(3.43) 21.08(3.92) 66.42(10.54)	5516.600(350) 3995.585(60) 2614.549(13)	3 ⁻ 4 ⁻ 3 ⁻	3.05(0.36)
113	6313.700(300)	1 ⁻	6313.70(30)	100.00	Ground state	0 ⁺	16.89(1.76)
114	6339.50(500)		3725.0(50)	100.00	2614.549(13)	3 ⁻	0.24(0.20)
115	6354.550(350)		2303.35(35)	100.00	4051.194(40)	3 ⁻	1.15(0.16)
116	6360.430(350)	1 ⁻	6360.43(35)	100.00	Ground state	0 ⁺	5.55(0.79)
117	6448.800(300)	13 ⁻	348.00(15) 1553.0(10)	83.00(4.00) 17.0(4.0)	6100.790(270) 4895.277(80)	12 ⁺ 10 ⁺	
118	6485.900(400)	1 ⁻ , 2 ⁻	512.98(25) 3871.70(70) 6486.0(12)	14.16(3.39) 14.75(8.85) 71.09(5.90)	5972.870(370) 2614.549(13) Ground state	2 ⁺ 3 ⁻ 0 ⁺	5.24(0.58)
119	6534.50(500)		3920.0(50)	100.00	2614.549(13)	3 ⁻	0.30(0.12)
120	6545.25(110)		3930.7(11)	100.00	2614.549(13)	3 ⁻	0.92(0.31)
121	6552.300(200)		3937.75(20) 6551.8(21)	100.00 14(1)	2614.549(13) Ground state	3 ⁻ 0 ⁺	11.80(1.30)
122	6617.250(350)	3 ⁻	2436.85(45) 4002.90(45)	33.76(7.07) 66.24(13.18)	4180.200(100) 2614.549(13)	5 ⁻ 3 ⁻	2.62(0.39)
123	6658.480(370)	4 ⁺	2478.70(50) 4043.50(50)	25.41(5.41) 74.59(10.59)	4180.200(100) 2614.549(13)	5 ⁻ 3 ⁻	3.51(0.42)
124	6682.800(300)	5 ⁻	2324.20(50) 2974.15(20) 4067.63(80)	32.10(7.41) 17.28(3.50) 50.62(7.61)	4358.785(63) 3708.511(43) 2614.549(13)	4 ⁻ 5 ⁻ 3 ⁻	4.27(0.48)

TABLE V. (Continued).

No.	$E_{\text{ini}}^{\text{level}}$ (keV)	I_{ini}^{π} (\hbar)	E_{γ} (keV)	I_{γ} (%)	$E_{\text{fin}}^{\text{level}}$ (keV)	I_{fin}^{π} (\hbar)	S_{expt} Relative
125	6699.850(250)	$1^{-}, 3^{-}$	1049.90(35) 2470.10(55) 4085.50(30)	15.64(3.96) 14.76(4.85) 69.60(5.07)	5649.700(280) 4229.620(50) 2614.549(13)	5^{-} 2^{-} 3^{-}	3.27(0.26)
126	6716.250(400)		6716.25(40)	100.00	Ground state	0^{+}	2.92(0.63)
127	6744.100(400)	14^{-}	295.30(25) 1508.1(10)	40.00(4.0) 60.0(6.0)	6448.800(300) 5235.440(180)	13^{-} 11^{+}	
128	6766.70(100)		4152.1(10)	100.00	2614.549(13)	3^{-}	1.03(0.28)
129	6773.40(150)		6773.4(15)	100.00	Ground state	0^{+}	0.67(0.59)
130	6789.150(600)	2^{-}	4174.60(60)	100.00	2614.549(13)	3^{-}	2.48(0.50)
131	6820.200(400)	2^{+}	872.20(70) 2873.75(40)	53.96(35.97) 46.04(9.35)	5947.460(450) 3946.620(100)	1^{-} 4^{-}	2.41(0.90)
132	6897.650(400)		2188.10(50) 2668.10(50)	34.39(8.99) 65.61(11.11)	4709.490(250) 4229.620(50)	5^{-} 2^{-}	1.63(0.23)
133	6920.750(800)		4306.20(80)	100.00	2614.549(13)	3^{-}	0.64(0.23)
134	6929.650(450)	2^{-}	4315.12(45)	100.00	2614.549(13)	3^{-}	4.16(0.71)
135	6969.420(450)		3771.68(45)	100.00	3197.740(13)	5^{-}	1.17(0.20)
136	7001.200(400)		3803.45(40)	100.00	3197.740(13)	5^{-}	1.68(0.24)
137	7020.250(400)	$1^{-}, 3^{-}$	1052.34(60) 2660.30(60) 2696.70(70) 2758.60(70)	15.88(4.54) 42.14(8.10) 18.64(4.70) 23.34(5.67)	5968.600(60) 4358.785(63) 4323.930(130) 4262.000(55)	4^{-} 4^{-} 4^{+} 4^{-}	5.20(0.62)
138	7063.400(500)	1^{-}	7063.40(50)	100.00	Ground state	0^{+}	5.16(1.04)
139	7080.60(200)	$1^{-}, 2^{-}$	7080.6(20)	100.00	Ground state	0^{+}	1.31(0.26)
140	7137.350(400)		4522.80(40)	100.00	2614.549(13)	3^{-}	2.31(0.47)
141	7196.70(100)	3^{-}	4582.1(10)	100.00	2614.549(13)	3^{-}	2.37(0.95)
142	7206.900(500)		7206.90(50)	100.00	Ground state	0^{+}	1.73(0.50)
143	7215.70(500)		4018.0(50)	100.00	3197.740(13)	5^{-}	
144	7238.700(600)	1^{-}	7238.70(60)	100.00	Ground state	0^{+}	0.15(0.08)
145	7264.40(100)	$3^{-}, 4^{-}$	4066.6(10)	100.00	3197.740(13)	5^{-}	10.37(1.71)
146	7315.40(200)	$2^{+}, 3^{+}$	7315.4(20)	100.00	Ground state	0^{+}	3.02(0.58)
147	7332.400(800)	1^{-}	7332.40(80)	100.00	Ground state	0^{+}	1.03(0.27)
148	7389.10(100)	$1^{-}, 3^{-}$	3914.0(10)	100.00	3475.103(15)	4^{-}	3.03(0.30)
							3.41(0.48)

26: This is a questionable level, it has been placed by the authors based on the γ transition seen in [7].

28,29: These states form a so far unresolved doublet. The spins are based on the γ decay and $l=2$ in $(d, {}^3\text{He})$ [6]. 32: Questionable state, based only on one weak γ transition in (d, p) .

34: Reference [24].

47: Questionable level, as the 2520 keV γ line is only a shoulder of the strong 2513 keV line from level 46.

53: Reference [8].

54: Reference [23].

61: Spin from [1] for a 5321(4) keV level.

63: Spin from [1] for a 5347.8(5) keV level.

67: Spin from [1] for a 5483(3) keV level.

70: Spin from [1] for a 5516.8(7) keV level.

82: Spin From [1] for a 5690(2) keV level.

84: Spin from [1] for a 5712(3) keV level.

85: Reference [25].

89: Spin from [1] for a 5805.0(15) keV level.

90: 3^{-} assignment in [1] for a state at 5813(4) keV.

92: From [1].

100: Spin from [1] for a 5973(20) keV level.

106: References [8,25].

117: Reference [8,25].

118: Spin from [1] for a 6485(4) keV level.

122: Spin from [1] for a 6615(2) keV level.

123: Spin from [1] for a 6658(5) keV level.

127: References [8,25].

134: Spin from [1] for a 6929(3) keV level.

138: Spin from [1] for a 7063.5(3) keV level.

139: Spin from [1] for a 7083.4(3) keV level.

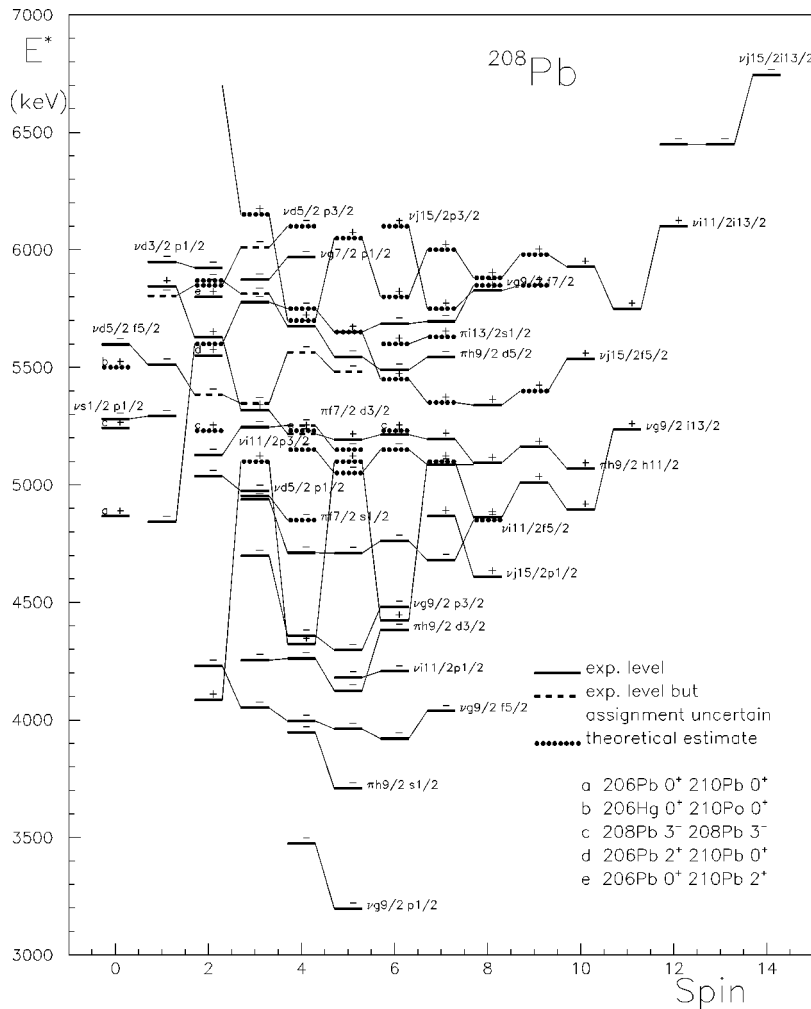


FIG. 5. Levels in ^{208}Pb ordered by spin. The single-particle–single-hole states below 6 MeV are shown. They are identified by their main configuration. As far as they are known, the experimental level energies are used (thick lines). Experimental states that likely belong to the indicated spin and configuration, but with uncertain spin assignments, are indicated by thin lines. For unknown states (dotted line) the theoretically expected energy is given. Also included are the low lying two-particle–two-hole states of particular structure as indicated. This figure is originally from Jan Blomqvist, Stockholm [26] and updated with the present experimental information.

some spin assignments, and assigned new spins and parities. Also very precise excitation energies (usually ≤ 0.1 keV) were determined, that might provide calibrations for other experiments and help to correlate states seen in different experiments. Spectroscopic factors have been determined for both proton pickup and neutron transfer, often resolving previously unresolved multiplets or detecting (for the first time) weakly populated levels. The parallel studies of γ transitions following inelastic heavy ion scattering [8,25] have extended the level scheme close to the Yrast line.

Particularly noteworthy is the clarification of misleading results from unresolved multiplets. The experimental information is now reliable, and the amount of data on spectroscopic factors and γ transitions is sufficient to derive empirical shell model wave functions. This evaluation will be presented in a separate work [16]; some selected results have already been published [14,22]. The matrix elements of the residual interaction can then be calculated from the wave functions by inverting the Schrödinger equation. These matrix elements can then be used to calculate the properties of other states in ^{208}Pb and neighboring nuclei. More important,

this experimentally determined interaction offers a test for any realistic interactions, that are calculated from the free nucleon-nucleon interaction.

Although there is now a one-to-one correspondence between the experimental states and those predicted by the shell model below $E_x = 4.5$ MeV, many states that the shell model demands below 6 MeV excitation energy have not yet been identified. Only the 0^+ member of the two octupole phonon multiplet has been found recently [23]. The technical means are now at hand to apply the (known) experimental methods to the study of ^{208}Pb at high excitation energy. ^{208}Pb is the most appropriate heavy doubly magic nucleus to explore the shell model, because it can be studied by a variety of reactions as it itself and some neighboring nuclei are stable.

We want to thank Jan Blomqvist, Stockholm, for many very valuable discussions and H.-G. Bohlen, HMI, for help and advice with the DWBA calculations. This work was supported by a grant of the NATO scientific cooperation program.

- [1] M. J. Martin, Nucl. Data Sheets **47**, 797 (1986).
- [2] W. T. Wagner, G. M. Crawley, G. R. Hammerstein, and H. Mcmanus, Phys. Rev. C **12**, 757 (1975).
- [3] P. B. Vold, J. O. Andreassen, J. R. Lien, A. Graue, E. R. Cosman, W. Dünneweber, D. Schmitt, and F. Nusslin, Nucl. Phys. **A215**, 61 (1973).
- [4] D. J. Horen, private communication to M. J. Martin, cited in M. J. Martin, Nucl. Data Sheets **47**, 797 (1986).
- [5] J. P. Connelly, D. J. de Angelis, J. H. Heisenberg, F. W. Hersman, W. Kim, M. Leuschner, T. E. Millimann, J. Wise, and C. N. Papanicolas, Phys. Rev. C **45**, 2711 (1992); J. P. Connelly, Ph.D. thesis, University of New Hampshire, 1989.
- [6] P. Grabmayr, G. Mairle, U. Schmidt-Rohr, G. P. A. Berg, J. Meissburger, P. von Rossen, and J. L. Tain, Nucl. Phys. **A469**, 285 (1987).
- [7] L. I. Govor, A. M. Demidov, and V. A. Kurkin, Bull. Acad. Sci. USSR, Phys. Ser. **54**, 147 (1990).
- [8] M. Schramm, H. Grawe, J. Heese, H. Kluge, K. H. Maier, R. Schubart, R. Broda, J. Grebosz, W. Krolas, A. Maj, and J. Blomqvist, Z. Phys. A **344**, 363 (1993).
- [9] M. Kortelahti, A. Pakkanen, and J. Kantele, Nucl. Phys. **A240**, 87 (1975).
- [10] E. Radermacher, M. Wilhelm, S. Albers, J. Eberth, N. Nicolay, H.-G. Thomas, H. Tiesler, P. von Brentano, R. Schwengner, S. Skoda, G. Winter, and K. H. Maier, Nucl. Phys. **A597**, 408 (1996).
- [11] E. D. Earle, A. J. Ferguson, G. van Middelkoop, G. A. Bartholomew, and I. Bergqvist, Phys. Lett. **32B**, 471 (1970).
- [12] N. Roy, K. H. Maier, A. Aprahamian, J. A. Becker, D. J. Decman, E. A. Henry, L. G. Mann, R. A. Meyer, W. Stöfl, and G. L. Struble, Phys. Lett. B **221**, 6 (1989).
- [13] M. Schramm, Ph.D. thesis, Freie Universität Berlin, 1993; Hahn-Meitner-Institut Report B-508, 1993.
- [14] M. Schramm, M. Rejmund, K. H. Maier, H. Grawe, and J. Blomqvist, Phys. Scr. **T56**, 307 (1995).
- [15] M. Rejmund, Diploma thesis, Warsaw University, 1995, unpublished.
- [16] K. H. Maier, M. Rejmund, and M. Schramm (unpublished).
- [17] S. Hinds, R. Middleton, J. H. Bjerregaard, O. Hansen, and O. Nathan, Phys. Lett. **17**, 302 (1965).
- [18] L. G. Mann, K. H. Maier, A. Aprahamian, J. A. Becker, D. J. Decman, E. A. Henry, R. A. Meyer, N. Roy, W. Stöfl, and G. L. Struble, Phys. Rev. C **38**, 74 (1988).
- [19] M. H. MacFarlane and S. C. Pieper, A program for heavy-ion direct-reaction calculations, Argonne National Laboratory, 1978.
- [20] J. J. van der Merwe, G. Heymann, Z. Phys. **220**, 130 (1969).
- [21] C. M. Perey, F. G. Perey, Nucl. Data Tables **10**, 539 (1972).
- [22] K. H. Maier, Acta Phys. Pol. B **28**, 277 (1997).
- [23] Minfang Yeh, P. E. Garrett, C. A. McGrath, and S. W. Yates, Phys. Rev. Lett. **76**, 1208 (1996).
- [24] R. Julin, J. Kantele, J. Kumpulainen, M. Luontama, A. Passoja, W. Trzaska, E. Verho, and J. Blomqvist, Phys. Rev. C **36**, 1129 (1987).
- [25] R. Broda, J. Wrzesinski, T. Pawlat, B. Fornal, Z. Grabowski, D. Bazzacco, S. Lunardi, C. Rossi-Alvarez, G. de Angelis, A. Gadea, and K. H. Maier, in Proceedings of the Conference on Nuclear Structure at the Limits, Argonne, Illinois, 1996 (unpublished), p. 276, ANL/PHY-97/1.
- [26] Jan Blomqvist, private communication.